Available online at www.sciencedirect.com
ScienceDirect
Trans. Nonferrous Met. Soc. China 22(2012) 2477−2483
Transactions of Nonferrous Metals Society of China
www.tnmsc.cn

Preparation of spherical activated carbon-supported and Er^{3+}:$YAlO_3$-doped TiO_2 photocatalyst for methyl orange degradation under visible light

DONG Shuang-shi, ZHANG Jian-bin, GAO Lin-lin, WANG Yan-long, ZHOU Dan-dan

Key Laboratory of Groundwater Resources and Environment, Ministry of Education, Jilin University, Changchun 130021, China

Received 9 July 2012; accepted 6 August 2012

Abstract: In order to develop the high photocatalytic activity of TiO_2 under visible light as that under ultraviolet light and make it easy to be separated from treated liquor, a visible light response and spherical activated carbon (SAC) supported photocatalyst doped with upconversion luminescence agent Er^{3+}:$YAlO_3$ was prepared by immobilizing Er^{3+}:$YAlO_3$/TiO_2, which was obtained by combination of Er^{3+}:$YAlO_3$ and TiO_2 using sol-gel method, on the surface of SAC. The crystal phase composition, surface structure and element distribution, and light absorption of the new photocatalysts were examined by X-ray diffraction (XRD), energy dispersive X-ray spectra (EDS) analysis, scanning electron microscopy (SEM) and fluorescence spectra analysis (FSA). The photocatalytic oxidation activity of the photocatalysts was also evaluated by the photodegradation of methyl orange (MO) in aqueous solution under visible light irradiation from a LED lamp (λ>400 nm). The results showed that Er^{3+}:$YAlO_3$ could perform as the upconversion luminescence agent which converts the visible light up to ultraviolet light. The Er^{3+}:$YAlO_3$/TiO_2 calcinated at 700 °C revealed the highest photocatalytic activity. The apparent reaction rate constant could reach 0.0197 min^{-1} under visible light irradiation.

Key words: visible light; upconversion luminescence; TiO_2; activated carbon; photocatalysis

1 Introduction

TiO_2 was firstly reported by Fujishima and Honda in 1972 to be able to generate various reactive oxygen species in water such as hydroxyl radicals, hydrogen peroxide, superoxide radical anions, under UV irradiation [1]. Since then, TiO_2 has widely been investigated for photocatalytic degradation of organic pollutants because of its strong photoactive ability, high stability, non-toxicity and low cost [2,3]. Although the technique is gradually near the stage of preindustrial application, there are still fundamental problems concerning the efficiency of photocatalysis that need to be solved. TiO_2 is a high band gap (E_g≈3.2 eV) material that can only be excited by high energy UV radiation with a wavelength of no longer than 387.5 nm [4]. But the content of UV in sunlight is only 3%−4%. Consequently, it limits the use of sunlight as an energy source. Although some investigations have reported that TiO_2 doped with non-metallic and metallic elements can achieve photocatalytic capacity under visible light [2,5,6], a low rate of electron transfer to oxygen and a high rate of recombination between electron/hole pairs result in a low quantum yield rate and also a limited photooxidation rate [7].

The upconversion luminescence agents such as Er^{3+}:$YAlO_3$ can transform the visible light into UV [8,9]. Thus, some researchers prepared TiO_2 doped with upconversion luminescence agents, and this sample can absorb visible light and excite ultraviolet. As a result, the photocatalytic activity of TiO_2 is improved under visible light [10,11].

TiO_2 powder has high catalytic activity, however, some limitations are discovered for the tiny powder in the sewage treatment, such as, easy to harden, difficult to settle, and difficult to recycle. The technology loaded TiO_2 to other material (quartz glass [12], ceramic [13] and activated carbon (AC) [14]) can well solve this problem. The presence of AC helps TiO_2 in contact with high concentration of pollutants because of its strong adsorption capacity, and improve the transfer rate of the interfacial charge and reduce the recombination rate of holes and electrons. Therefore, the photocatalytic

Foundation item: Projects (50908096, 50908097) supported by the National Natural Science Foundation of China; Project (20100471251) supported by China Postdoctoral Science Foundation
Corresponding author: ZHOU Dan-dan; Tel: +86-431-88499792; E-mail: zhoudandan415@163.com
DOI: 10.1016/S1003-6326(11)61488-X

efficiency of TiO_2 is improved [15].

In this study, a visible light response and spherical activated carbon (SAC) supported photocatalyst doped with Er^{3+}:$YAlO_3$ (Er^{3+}:$YAlO_3$/TiO_2-SAC) was prepared. The compound Er^{3+}:$YAlO_3$, combining erbium, yttrium and aluminum, could function as an upconversion luminescence for photo-exciting TiO_2 under visible light. The Er^{3+}:$YAlO_3$-doped TiO_2 loaded on the spherical activated carbon particles could be a photocatalyst that would provide dramatically photocatalytic degradation of organic pollutants under visible-light irradiation, and could be easy to settle out of the treated liquor. The prepared photocatalyst was also characterized and evaluated by surface analysis and photocatalytic activity tests, respectively.

2 Experimental

2.1 Catalyst preparation

2.1.1 Preparation of Er^{3+}:$YAlO_3$ by nitrate-citric acid method

The Er^{3+}:$YAlO_3$ sample was prepared by nitrate-citric acid method following the steps described elsewhere [16,17]. $Al(NO_3)_3$ was dissolved into distilled water in a beaker and stirred for 1 h at room temperature. Then, $Y(NO_3)_3$ and $Er(NO_3)_3$ were completely dissolved in distilled water and added to the above solution under constant stirring. The molar ratio of Er, Y to Al was controlled at 0.01:0.99:1.00. Both solutions were mixed together and solid citric acid was added (molar ratio of citric acid metal ion 3:1). The final solution was evaporated at 85 °C on a water bath until a pale, translucent and viscous gel was formed. The obtained gel was dried at 130 °C for 24 h followed by dispersion to obtain a powder. The sample was calcinated at 1200 °C in a muffle furnace for 2 h. After grinding, the nanocrystalline Er^{3+}:$YAlO_3$ powder was obtained.

2.1.2 Preparation of Er^{3+}:$YAlO_3$/TiO_2 by sol-gel method

The Er^{3+}:$YAlO_3$/TiO_2 was prepared via the sol-gel method. The molar ratio of $Ti(OC_4H_9)_4$:C_2H_5OH:H_2O:CH_3COOH was controlled at 1:10:2:1 and the final quality ratio of (Er^{3+}:$YAlO_3$):TiO_2 was controlled at 1:10. $Ti(OC_4H_9)_4$ was added dropwise into half of the total amount of C_2H_5OH and then the solution was stirred for 30 min at room temperature. The obtained solution was named as solution A. Subsequently, Er^{3+}:$YAlO_3$, CH_3COOH, H_2O and another half of the C_2H_5OH were mixed together and stirred for 30 min. Then, solution B was obtained. Afterwards, the solution B was added dropwise into the solution A with vigorous stirring and the final solution was continuously stirred at 40 °C for 2 h. After aging for 48 h, titania gel was formed on the surface of the Er^{3+}:$YAlO_3$ particles, followed by drying at 110 °C for 24 h. The obtained dry sample was ground and calcinated at 500, 600, 700 and 800 °C for 2 h, with a heating rate of 5 °C /min.

2.1.3 Preparation of Er^{3+}:$YAlO_3$/TiO_2-SAC

The mass ratio of (Er^{3+}:$YAlO_3$/TiO_2) to SAC was 1:4. Er^{3+}:$YAlO_3$/TiO_2 was dispersed in the appropriate anhydrous ethanol with ultrasonic treatment for 30 min. The spherical activated carbon (SAC, 0.6 mm in diameter, Kureha Corp, Japan) was added into the above mixture and stirred for 1 h. The sample was dried at 70 °C after standing for 24 h, and then, the dry sample was heat-treated at 300 °C for 1 h. The final sample of Er^{3+}:$YAlO_3$/TiO_2-SAC was the photocatalyst used for characterization and photocatalytic performance examination.

2.2 Photocatalytic degradation of methyl orange

Methyl orange (MO) was selected as the model pollutant to examine the photocatalytic activity of Er^{3+}:$YAlO_3$/TiO_2-SAC. 1 g of photocatalyst was added to 50 mL of 1000 mg/L MO solution. MO adsorption by catalyst particles for 24 h was conducted before photocatalytic degradation, and the residual MO concentration was (136±8) mg/L. The solution was irradiated by an 18 W-LED lamp from top with surface aeration by air flow of 0.6 L/min to obtain a uniform distribution of MO concentration. Figure 1 shows the emission spectrum of the lamp, with two strong peaks at 455.0 nm and 552.9 nm. UV was not detected, verified by a UV meter (TN-2234UVC, TAINA, Taiwan, China). The MO concentration was determined by an UV-vis spectrophotometer at 460 nm. All the experiments were carried out in a dark chamber to avoid interference of ambient light on the photoreaction.

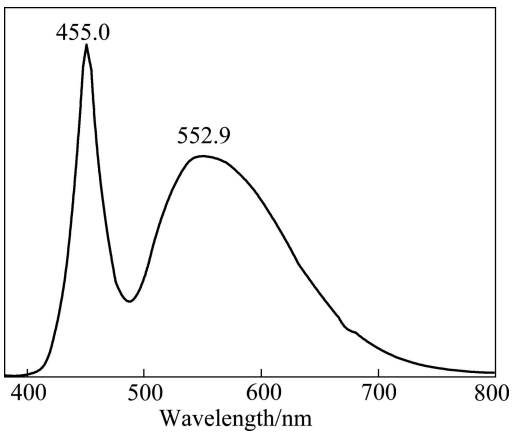

Fig. 1 Light spectrum of LED lamp

3 Results and discussion

3.1 Photocatalyst characterization

3.1.1 SEM and EDS analyses

SEM and EDS analyses were performed by a

scanning electron microscope (Quanta 200 ESEM, FEI, USA) in order to examine the morphology and elemental contents of the samples. The SEM image of the Er^{3+}:$YAlO_3$/TiO_2-SAC showed the fairly uniform distribution of Er^{3+}:$YAlO_3$/TiO_2 (calcinated at 700 °C) on the surface of SAC. This indicated a strong attachment of the Er^{3+}:$YAlO_3$/TiO_2 particles onto SAC. According to the EDS element mapping, it was evident that all the dopant elements, including Er, Y and Al, were observed on the surface of SAC. Additionally, the distribution of Ti corresponded to the white clouds in the SEM image and the distribution of C to the black clouds, respectively. The detected molar ratios (Fig. 3) showed that C occupied more than 96% of the total amount and the result suggested that immobilized Er^{3+}:$YAlO_3$/TiO_2 would not cover all the surface of SAC, which was helpful to MO adsorption onto the SAC surface and TiO_2 photocatalytic destruction.

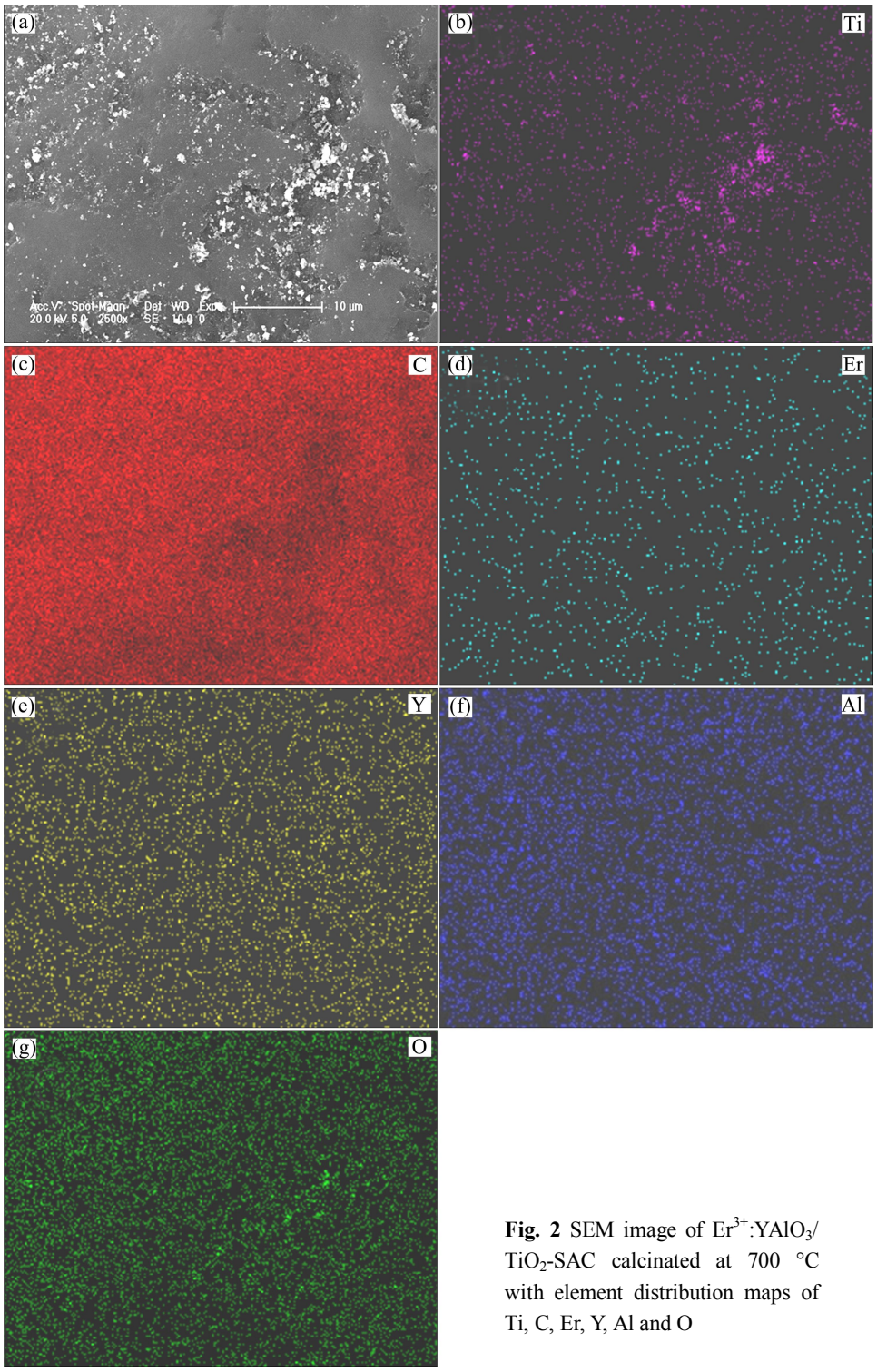

Fig. 2 SEM image of Er^{3+}:$YAlO_3$/TiO_2-SAC calcinated at 700 °C with element distribution maps of Ti, C, Er, Y, Al and O

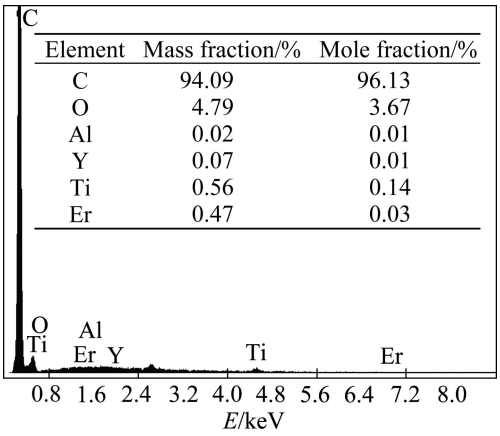

Fig. 3 EDS spectrum on surface of Er^{3+}:$YAlO_3$/TiO_2-SAC

3.1.2 XRD analysis

The XRD patterns of the samples were determined by powder X-ray diffractometer (RINT 2500, Rigaku Corporation, Japan) using Ni filtered Cu K_α radiation with the 2θ range from 10° to 90° at the scanning speed of 1 (°)/min. Figure 4 presents the XRD patterns of Er^{3+}:$YAlO_3$/TiO_2 calcinated at various temperatures. All Er^{3+}:$YAlO_3$/TiO_2 samples showed the strong peak at 25.4° corresponding to anatase TiO_2. In addition, the characteristic peak at 27.4° corresponding to the rutile phase was observed with the calcination temperature up to 800 °C, suggesting the transformation of anatase to rutile phase at this temperature.

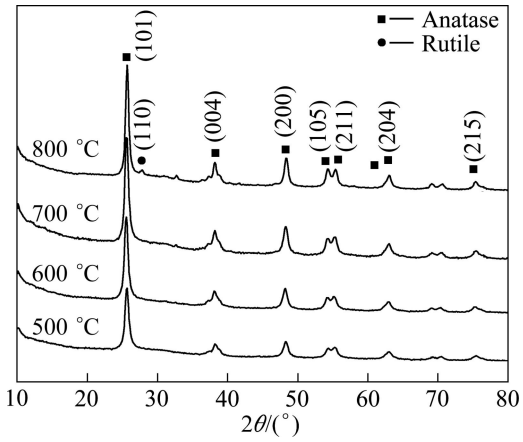

Fig. 4 XRD patterns of Er^{3+}:$YAlO_3$/TiO_2 calcinated at different temperatures

The mass fraction of anatase and rutile phases and the mean size of a single crystallite could be determined by Spurr-Myers equation [18] and Scherrer equation [19], respectively. The average crystallite sizes and the content of anatase and rutile phases of the synthesized catalysts calcinated at different temperatures are listed in Table 1. The crystallite size of TiO_2 in the composites slightly increased with the increase of calcination temperature, indicating that the heat treatment resulted in TiO_2 crystal growth and the presence of activated carbon baffles TiO_2 growth for the composite formation, as compared to the case of bare TiO_2 [20].

Table 1 Average crystallite size and contents of anatase and rutile in photocatalyst samples

Calcining temperature/°C	Average crystallite size/nm	Crystallite phase content/%	
		Anatase	Rutile
500	13.37	100	0
600	13.67	100	0
700	13.56	100	0
800	15.73	97.26	2.74

3.1.3 Fluorescence spectra analysis

The fluorescence spectra (Fig. 5) of Er^{3+}:$YAlO_3$ were obtained by a fluorescence spectrophotometer (Varian Cary Eclipse, USA). Two excitation wavelengths were selected according to the light spectrum of the LED lamp. Regarding to the 455 nm and 553 nm excitation, there were the upconversion emission wavelength of 360 nm and 320 nm as well as 362 nm, respectively, which were all shorter than 387 nm and could excite TiO_2 to generate e^-/h^+. On the other hand, the emission intensity

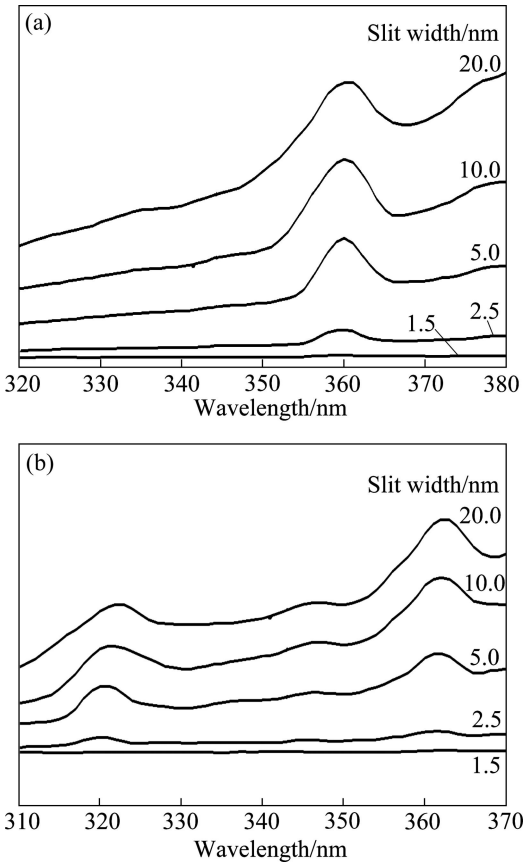

Fig. 5 Fluorescence spectra of Er^{3+}:$YAlO_3$ with excitation wavelength of 455 nm (a) and 553 nm (b)

increased with the increase of the slit width where excitation beam passed in the spectrophotometer, implying a two-step upconverted process taking place under the two photons excitations [9].

3.2 Photocatalytic activity of Er^{3+}:$YAlO_3/TiO_2$-SAC

Figure 6(a) shows a comparison between MO adsorption and MO photocatalytic degradation by Er^{3+}:$YFeO_3/TiO_2$-SAC with and without visible light irradiation. Without the visible light irradiation, the reduction of MO could be only attributed to its adsorption by SAC and the removal efficiency was 43.7% after 120 min. When the Er^{3+}:$YAlO_3/TiO_2$-SAC calcinated at 500, 600, 700 and 800 °C were irradiated by the LED, the MO removal efficiencies after 120 min reached 75.1%, 82.1%, 90.8%, and 85.1%, respectively. It was evident that when the photocatalysts were irradiated by the visible light, the decreasing rates of MO concentration were much higher than that without visible light irradiation, indicating that MO was rapidly decomposed by the irradiated Er^{3+}:$YAlO_3/TiO_2$-SAC photocatalytically. Figure 6(b) presents the effect of calcination temperature on photocatalytic activity of Er^{3+}:$YAlO_3/TiO_2$-SAC for the degradation of MO under visible light irradiation. Compared to the sample in dark condition with the apparent reaction rate constant of 0.0052 min^{-1}, all the prepared photocatalysts irradiated by LED possessed much higher apparent reaction rate constant. The photocatalytic activity of Er^{3+}:$YAlO_3/TiO_2$-SAC could be enhanced by increasing calcination temperature from 500 °C to 700 °C. The apparent reaction rate constant increased from 0.0122 min^{-1} to 0.0197 min^{-1}. The calcination at relatively low temperature led to a lower crystallinity of anatase TiO_2 phase and the Er^{3+}:$YAlO_3/TiO_2$ was not well formed, which resulted in a lower photocatalytic activity of the Er^{3+}:$YAlO_3/TiO_2$-SAC. Meanwhile, previous study showed that anatase was more active than rutile in photocatalytic capacity [21], due to the fact that anatase was able to substantially ionosorb oxygen species, which were principally involved in electron capture in the aqueous phase reactions. Thus, the Er^{3+}:$YAlO_3/TiO_2$-SAC prepared at the calcination temperature of 800 °C showed a slight decrease in the photocatalytic activity due to the presence of rutile (Table 1).

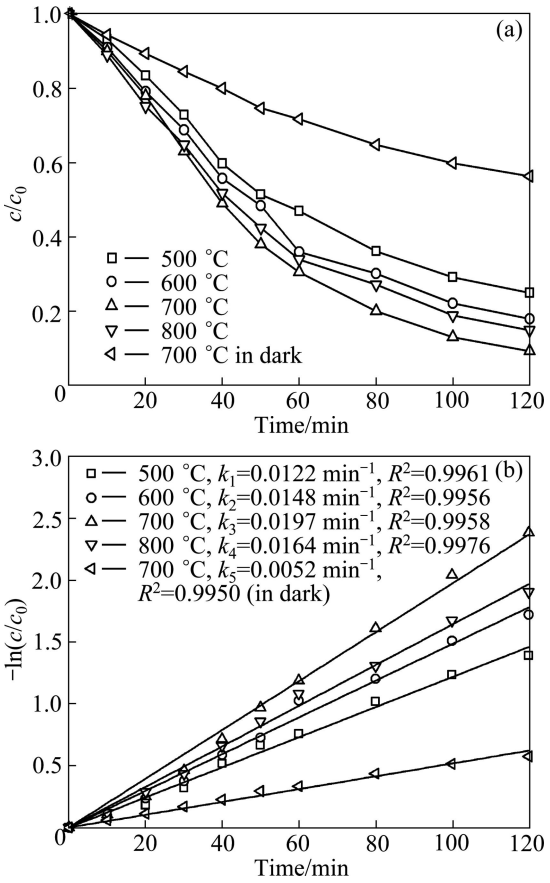

Fig. 6 Decrease in MO concentration (a) and linear plots of reaction kinetics (b) for Er^{3+}:$YAlO_3/TiO_2$-SAC calcinated at different temperatures

3.3 UV-vis spectra of MO solution during photocatalytic degradation

From the UV-vis absorption spectra of MO (Fig. 7), there was a large absorption peak at wavelength of 460 nm. Studies indicated that, this absorption peak was derived from the chromophore which was produced by the conjugated system composed of the azo bond and benzene ring [22], as seen in the inset of Fig. 7. The azo bond was attacked by photo-generated holes and/or free radicals which came from the photocatalytic degradation process, and the photocatalytic destruction of the C—N bond and the N—N bonds led to fading of the MO.

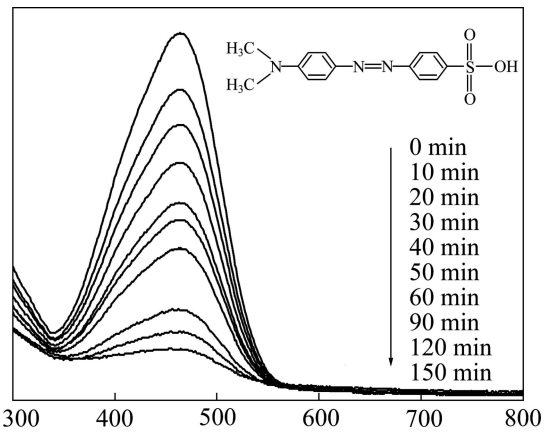

Fig. 7 Chemical structure and UV-vis spectra of MO in aqueous solution

3.4 Mechanism for MO degradation under visible light

As illustrated in Fig. 8, the activated carbon adsorbs MO from the solution and promotes its mass

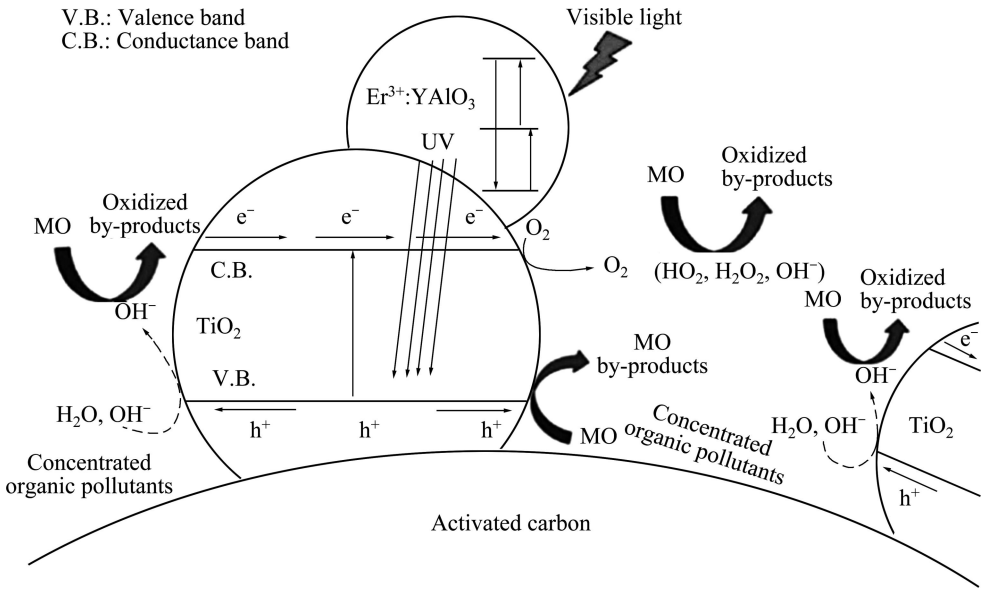

Fig. 8 Proposed photocatalytic mechanisms over Er^{3+}:$YAlO_3$/TiO_2 under visible light irradiation

transfer to the surface of the SAC-supported TiO_2 whereby various reactive oxidizing species were produced, resulting in the enhancement of photocatalytic degradation of MO. The crystallized Er^{3+}:$YAlO_3$ as upconversion luminescence agent firstly absorbs the incident pump visible light and then continuously emits UV by a two-step upconverted process. The UV can effectively excite the TiO_2 nanoparticles and result in the formation of photo-generated electron-hole pairs. In the similar way as general photocatalytic degradation, these holes not only directly decompose MO, but also oxidize water molecule to form highly oxidative radicals with high activity and indirectly degrade the MO in aqueous solution, resulting in destruction of the C—N bond and the N—N bond of the MO and formation of degradation by-products and mineral acids or complete mineralization into CO_2 and H_2O.

4 Conclusions

1) Er^{3+}:$YAlO_3$/TiO_2-SAC, an activated carbon-supported visible-light responsive photocatalyst, was prepared by means of ultrasonic dispersion and sol-gel method. The photocatalyst calcinated at 700 °C, exhibited the highest photocatalytic activity under visible light irradiation.

2) In the composite photocatalyst, the Er^{3+}:$YAlO_3$ acted as an upconversion luminescence agent to convert visible light into UV for photoexcitation of the TiO_2, while the activated carbon acted as pollutant-concentrating photocatalyst support. This combined functionality could enhance MO removal from liquid phase. The destruction of C—N bond and N—N bond by photocatalytic oxidation led to the destruction of MO.

References

[1] FUJISHIMA A, HONDA K. Electrochemical photolysis of water at a semiconductor electrode [J]. Nature, 1972, 238(7): 37−38.

[2] LI X Z, LI F B. Study of Au/Au^{3+}-TiO_2 photocatalysts toward visible photooxidation for water and wastewater treatment [J]. Environ Sci Technol, 2001, 35(11): 2381−2387.

[3] CHONG M N, JIN B, CHOW C W K, SAINT C. Recent developments in photocatalytic water treatment technology: A review [J]. Water Res, 2010, 44(10): 2997−3027.

[4] GOSWAMI D Y. A review of engineering developments of aqueous phase solar photocatalytic detoxification and disinfection processes [J]. J Sol Energ-T ASME, 1997, 119(3): 101−107.

[5] DONG F, WANG H Q, SEN G, WU Z B, LEE S C. Enhanced visible light photocatalytic activity of novel Pt/C-doped TiO_2/$PtCl_4$ three-component nanojunction system for degradation of toluene in air [J]. J Hazard Mater, 2011, 187(1−3): 509−516.

[6] ILIEV V, TOMOVA D, RAKOVSKY S. Nanosized N-doped TiO_2 and gold modified semiconductors–photocatalysts for combined UV-visible light destruction of oxalic acid in aqueous solution [J]. Desalination, 2010, 260(1−3): 101−106.

[7] LINSEBIGLER A L, LU G, YATES J T. Photocatalysis on TiO_2 surfaces: Principles, mechanisms, and selected results [J]. Chem Rev, 1995, 95(3): 735−758.

[8] YANG Hai-gui, DAI Zhen-wen, SUN Zhi-wei. Upconversion luminescence and kinetics in Er^{3+}:$YAlO_3$ under 652 nm excitation [J]. J Lumin, 2007, 124(2): 207−212.

[9] XU Huai-liang, JIANG Zhan-kui. Dynamics of visible-to-ultraviolet upconversion in $YAlO_3$:1% Er^{3+} [J]. Chem Phys, 2003, 287(1−2): 155−159.

[10] WANG Jun, MA Teng, ZHANG Guan, ZHANG Zhao-hong, ZHANG Xiang-dong, JIANG Yue-feng, ZHAO Gang, ZHANG Peng. Preparation of novel nanometer TiO_2 catalyst doped with upconversion luminescence agent and investigation on degradation of acid red B dye using visible light [J]. Catal Commun, 2007, 8(3): 607−611.

[11] GAO Jing-qun, LUAN Xiao-yu, WANG Jun, WANG Bao-xin, LI Kai, LI Ying, KANG Ping-li, HAN Guang-xi. Preparation of Er^{3+}:$YAlO_3$/Fe-doped TiO_2-ZnO and its application in photocatalytic

degradation of dyes under solar light irradiation [J]. Desalination, 2011, 268(1−3): 68−75.

[12] ZHANG Zhi-hong, ZHANG Hai-ming, WU Lian-ping, HAN Yang, ZHAO Lian-hua. The photocatalytic activity of prepared TiO_2 thin films on various glass substrates [J]. Journal of Yanbian University, 2008, 34(2): 131−134. (in Chinese)

[13] KANKI T, HAMASAKI S, SANO N, TOYODA A, HIRANO K. Water purification in a fluidized bed photocatalytic reactor using TiO_2-coated ceramic particles [J]. Chem Eng J, 2005, 108(1−2): 155−160.

[14] GUO Yan-hong. Photocatalytic degradation of phenol in wastewater over titania supported on activated carbon [J]. Industrial Catalysis, 2006, 14(6): 42−45.

[15] LIM T T, YAP P S, SRINIVASAN M, FANE A G. TiO_2/AC composites for synergistic adsorption-photocatalysis processes: Present challenges and further developments for water treatment and reclamation [J]. Environ Sci Technol, 2011, 41(13): 1173−1230.

[16] TANNER, P A, LAW P T, WONG K L, FU L S. Preformed sol-gel synthesis and characterization of $YAlO_3$ [J]. J Mater Sci, 2003, 38(24): 4857−4861.

[17] WANG Jun, LI Jia, LIU Bin, XIE Ying-peng, HAN Guang-xi, LI Ying, ZHANG Li-qun, ZHANG Xiang-dong. Preparation of nano-sized mixed crystal TiO_2-coated Er^{3+}:$YAlO_3$ by sol-gel method for photocatalytic degradation of organic dyes under visible light irradiation [J]. Water Sci Technol, 2009, 60(4): 917−926.

[18] SPURR R A, MYERS H. Quantitative analysis of anatase-rutile mixtures with an X-ray diffractometer [J]. Anal Chem, 1957, 29(5): 760−762.

[19] DEMEESTERE K, DEWULF J, OHNO T, SALGADO P H, LANGENHOVE H V. Visible light mediated photocatalytic degradation of gaseous trichloroethylene and dimethyl sulfide on modified titanium dioxide [J]. Appl Catal B Environ, 2005, 61(1−2): 140−149.

[20] LI You-ji, ZHANG Shi-ying, YU Qu-min, YIN Wen-bin. The effects of activated carbon supports on the structure and properties of TiO_2 nanoparticles prepared by a sol-gel method [J]. Appl Surf Sci, 2007, 253(23): 9254−9258.

[21] SCLAFANI A, HERRMANN J M. Comparison of the photoelectronic and photocatalytic activities of various anatase and rutile forms of titania in pure liquid organic phases and in aqueous solutions [J]. J Phys Chem, 1996, 100(32): 13655−13661.

[22] DING Hon-grui, LI Yan, LU An-huai, JIN Song, QUAN Chao, WANG Chang-qiu, WANG Xin, ZENG Cuiping, YAN Yun-hua. Photocatalytically improved azo dye reduction in a microbial fuel cell with rutile-cathode [J]. Bioresource Technol, 2010, 101(10): 3500−3505.

球形活性炭负载和 Er^{3+}:$YAlO_3$ 掺杂 TiO_2 的制备及其在可见光下降解甲基橙

董双石，张建宾，高琳琳，王艳龙，周丹丹

吉林大学 地下水资源与环境教育部重点实验室，长春 130021

摘 要：为使 TiO_2 能够在可见光下发挥其于紫外激发下的高光催化活性，且易于从处理废水中分离，采用溶胶−凝胶法将 TiO_2 与掺杂稀土离子 Er^{3+}的上转换发光剂 Er^{3+}:$YAlO_3$ 结合，再将其负载到球形活性炭(SAC)表面，制备出可见光响应的负载型 Er^{3+}:$YAlO_3$/TiO_2-SAC 光催化剂。通过 XRD、EDS、SEM 与 FSA 等手段对制备的光催化剂进行晶相、表面结构与元素分布、发光光谱等表征。以甲基橙为目标污染物，研究制备的光催化剂在可见光下的催化活性。结果表明，Er^{3+}:$YAlO_3$ 可以作为上转换发光材料，它吸收可见光并发射紫外光进而激发 TiO_2。700 °C 煅烧制备的催化剂具有最佳的光催化活性，可见光下表观反应速率常数可达 0.0197 min^{-1}。

关键词：可见光；上转换发光材料；TiO_2；活性炭；光催化

(Edited by YUAN Sai-qian)